LBNL-55344

An *in-situ* cell for characterization of solids by soft X-ray absorption

Running Title: *In-Situ* cell for soft X-ray absorption

Ian J. Drake,[a)] Teris C.N. Liu,[a,b)] Mary Gilles,[c)] Tolek Tyliszczak,[c)]
A.L.David Kilcoyne,[d)] David K. Shuh,[c)] Richard.A. Mathies,[b)]
Alexis T. Bell [a,c,*)]

[a)] Department of Chemical Engineering, University of California, Berkeley, CA 94720-1462

[b)] Department of Chemistry, University of California, Berkeley, CA 94720-1461

[c)] Chemical Sciences Division, Lawrence Berkeley National Laboratory, Berkeley, CA 94720.

[d)] Advanced Light Source, Lawrence Berkeley National Laboratory, Berkeley, CA 94720

(Received 15 March 2004)

(Revised 29 June 2004)

Review of Scientific Instruments

[*] To whom correspondence should be addressed
Tel: 510-642-1536. Fax: 510-642-4778. E-mail: bell@cchem.berkeley.edu

Abstract

An *in-situ* cell using "lab-on-a-chip" technologies has been designed and tested for characterization of catalysts and environmental materials using soft X-ray absorption spectroscopy and spectromicroscopy at photon energies above 250 eV. The sample compartment is 1.0 mm in diameter with a gas path length of 0.8 mm to minimize X-ray absorption in the gas phase. The sample compartment can be heated to 533 K by an Al resistive heater and gas flows up to 5.0 cm^3 min^{-1} can be supplied to the sample compartment through microchannels. The performance of the cell was tested by acquiring Cu L_3-edge XANES data during the reduction and oxidation of a silica-supported Cu catalyst using the beam line 11.0.2 Scanning Transmission X-ray Microscope (STXM) at the Advanced Light Source of LBNL. Two-dimensional images of individual catalyst particles were recorded at photon energies between 926 eV and 937 eV, the energy range in which the Cu(II) and Cu(I) L_3 absorption edges are observed. Oxidation state specific images of the catalyst clearly show the disappearance of Cu(II) species during the exposure of the oxidized sample to 4% CO in He while increasing the temperature from 308 K to 473 K. Reoxidation restores the intensity of the image associated with Cu(II). L-edge XANES spectra obtained from stacks of STXM images show that with increasing temperature the Cu(II) peak intensity decreases as the Cu(I) peak intensity increases.

Keywords: *In-Situ* **XAS, Cu L_3 edge XANES, Soft X-ray absorption, *In-situ* cell, microfluidics**

Introduction

X-ray absorption spectroscopy (XAS) is a powerful tool for characterizing finely divided materials such as catalysts, solid pollutants, and soils.[1,2] Information about the bulk or near-surface oxidation state of a solid is obtained from either X-ray photoelectron spectroscopy (XPS) or X-ray absorption near edge structure (XANES) spectroscopy. Additionally, the local coordination of an element in a solid can be obtained from extended X-ray absorption fine structure (EXAFS) spectroscopy.[2-5]

XPS measurements can be made with both laboratory X-ray sources and synchrotron radiation (SR) sources; however, the latter source offers the advantage of a wide range of tunable energies and very high photon fluxes. Since the local structure and composition of many solids are sensitive to the temperature and composition of the surrounding environment, there is considerable motivation for conducting *in-situ* XAS measurements as well as complimentary XPS experiments.[5] A variety of *in-situ* cells using transmission or fluorescence techniques have been described for acquiring XAS data with hard X-rays (3,500-35,000 eV).[6] Due to long attenuation lengths in this energy range, the size of the *in-situ* cell is not an issue. An *in-situ* XAS cell designed for catalyst studies in the intermediate energy range of 1000-3500 eV has also been reported.[7] XAS data are collected by either fluorescence or electron-yield detection at pressures of 10^{-4} atm to 1 atm and temperatures of 80 K to 750 K. While this apparatus has proven useful for studying the K-edge of metals such as Mg, Al, and Si, there is a growing interest in exploring electronic transitions occurring below 1000 eV.[8,9] This range includes the K-edge of low Z elements $6<Z<10$ such as oxygen and the L-edge of 3d and M-edge of 4d

transition metals. Recently, two apparatus capable of *in-situ* experiments in the range of 250-1000 eV were described.[10, 11] Both systems rely on electron rather than photon detection and are currently limited to pressures below 10 mbar; however, improvements that allow for operation up to 100 mbar were described.[11] The pressure limitation is due to the rapid attenuation of electrons in the gas surrounding the sample and the need to extract the electrons through a pinhole into the energy analyzer, which is maintained *in vacuo*. While this apparatus has opened the way for the *in situ* characterization of solids by XPS[3] and near edge X-ray absorption fine structure (NEXAFS) spectroscopy[4], there continues to be strong motivation for sample characterization at higher pressures.[12]

Recent developments in SR source brightness and flux, along with advances in photon detection, have made transmission experiments in the soft X-ray regime possible. In addition, the ability to generate highly focused X-ray beams has enabled two-dimensional elemental mapping of a sample .[13] The Scanning X-ray Transmission Microscopes (STXM) at the Advanced Light Source (ALS) were developed for this purpose and are capable of providing element and speciation specific micrographs with a spatial resolution of 25-40 nm in the photon energy range of 130-2000 eV.[14] Samples examined in the STXM are typically mounted on a 50 – 100 nm Si_3N_4 windowed silicon chip and placed in a chamber that can either be evacuated or filled with dry He. Data acquisition is normally done at ambient temperatures of the laboratory.

We describe a microreactor designed specifically for STXM soft X-ray studies above 250 eV that is operated under flow conditions, and at 1 atm total pressure and temperatures up to 533 K. This design extends the characterization of solid materials to realistic atmospheric pressure operating conditions.[10,11] Since the cell is designed for

transmission measurements, the type of material studied is not limited, as is the case for total electron yield measurements, to samples with adequate electrical conductance.[7] Hence, this cell can be used to characterize the O K-edge and the L edges or M edges of 3d or 4d transition metals, respectively, and their oxides supported on non-conducting supports.

Experimental

Four design objectives were identified to achieve *in-situ* characterization of a solid using soft X-rays in the range of 250 to 1000 eV. The first requirement is minimization of the optical pathlength in order to maximize the photon flux so that spectra can be collected with a reasonable signal to noise ratio. Second, the solid material to be characterized needs to be isolated from the ambient atmosphere by X-ray transparent windows so that a controlled atmosphere can be maintained around the sample. The third requirement is that it be possible to supply reactant gas to and from the cell. Finally, it must be possible to heat the sample compartment.

To achieve a minimal optical path length, the *in-situ* cell was fabricated on a glass wafer (0.55-mm thick, 100 mm diameter D263, Schott, Yonkers, NY) using microlithographic techniques at the UC Berkeley Microfabrication Laboratory (Microlab).[15] The flow channels were etched into the glass wafer following standard procedures. The surface of the wafer was cleaned before depositing an amorphous silicon layer (2000 Å) in a low-pressure chemical-vapor-deposition (LPCVD) furnace. The wafer was then primed with hexamethyldisilazane, spin-coated with photoresist (Shipley 1818, Shipley Company) at 2500 rpm, and soft-baked for 2.5 min at 393 K. The

pattern of the microfluidic channel and sample area (Figure 1a) were transferred to the substrate by exposing the photoresist to UV light with a Quintel UV contact mask aligner and subsequently developed in a 1:1 mixture of Microposit Concentrate (Shipley Company) and water. This exposed the features on the amorphous silicon layer to be etched. The mask pattern was transferred to the amorphous silicon by CF_4 plasma etching performed in a plasma-enhanced chemical vapor deposition (PECVD) system (PEII-A, Technics West, San Jose, CA). The exposed silica of the wafer was etched in 49% HF for 6 min at an etch rate of 35 μm/min, giving a final etch depth of 210 μm. Since the etching is isotropic, this gave a hydraulic diameter of the flow channels of approximately 260 μm. The exposed photoresist was then stripped using PRS3000 solution (aggressive organic solvent containing n-methyl pyrollidone) and the remaining amorphous silicon was removed by CF_4 plasma etching.

An aluminum resistive heater was fabricated on the wafer following completion of the flow channels. 5000 Å of Al was deposited on the back side of the glass wafer using a sputtering machine (CPA). This thickness was determined experimentally to provide adequate heating performance. The wafer was primed a second time with hexamethyldisilazane, spin-coated with photoresist (Shipley 1818, Shipley Company) at 2500 rpm, and then soft-baked for 2.5 min at 393 K. The heater pattern was transferred to the substrate by exposing the photoresist to UV light with a Karl Suss MA6 mask aligner. The photoresist was again developed in a 1:1 mixture of Microposit Concentrate (Shipley Company) and water. The excess aluminum was then etched in Aluminum Etchant Type A (Transene Co., Inc.) at 323 K at an etch rate of 6000 Å min^{-1}. The resistance of the heater (6 Ω) was optimized to provide heating with a 10 V power supply.

The heater leads were roughly 2.5 times wider than the heating element to ensure localized heating around the sample chamber.

Access holes of 1.5 mm diameter to the microfluidic channels, were then diamond drilled with a manual drill press. A closed channel was formed by irreversibly bonding the glass substrate to a 250 μm-thick polydimethylsiloxane (PDMS) membrane (Rogers Corporation). Prior to bonding the PDMS membrane, the surface of the wafer was activated by a UV-Ozone cleaner (Jelight company).[16] PDMS was chosen because it bonds easily to glass via this procedure, and is sufficiently tacky to help adhere the Si_3N_4 window chip. Nanoport connectors (Upchurch scientific) were used to ensure a leak-free connection between the microchannels and the external gas sources.

A detailed drawing of the cell is shown in Figure 1. Three identical cells were fabricated on a single 100 mm diameter glass wafer. The sample compartment has a diameter of 1.0 mm and a gas path length of 0.8 mm. The open ends of the sample compartment are closed by Si_3N_4 windows (Silson Ltd.). The window is 100 nm thick covering an area of 0.5 mm x 0.5 mm in a 5.0 mm frame and attached to the cell body by applying a high-temperature, tacky PDMS adhesive (DOW Corning 280A adhesive; trial sample) to the outer edge of each window. The adhesive does not requiring curing and can be used continuously up to 533 K. Furthermore, the Si_3N_4 windows can be removed making the cell entirely reusable.

A gas manifold was built to deliver up to four gases to the cell. The supply of each gas was enabled or disabled by the actuation of a miniature solenoid valve (Lee company HDI series 3-way valves). Gas flow was regulated up to 5.0 cm^3 min^{-1} with a fine adjustment needle valve with the pressure drop between entrance and exit of the *in-*

situ cell monitored by a miniature semiconductor transducer (Omega PX138) which was linearly proportional to the flow rate. As a result, the pressure drop across the reactor (typically ~ 1 psig) could be used to monitor the flow rate. Power for the Al heater was provided by a bipolar 15 V, 2 A power supply. The heater, pressure transducer, solenoid valves, and thermocouple were interfaced to a personal computer via an analog-to-digital/digital-to-analog board (NI PCI-6052E). A LabVIEW program was developed to monitor and control the temperature, the pressure drop across the cell and to switch gases.[17]

Results

The calculated absorption[18] characteristics of a 0.8 mm long gas cell are shown in Figure 2. In the absence of any gas, some absorbance at 410 eV occurs due to the nitrogen K-edge of the two 100 nm thick silicon nitride (Si_3N_4) windows. Introduction of a gas mixture containing 4% CO, 10% O_2 in a background of He leads to an increase in the absorbance associated with C and O K-edge features. Increasing the concentrations of these gases by a factor of five, increases the C, N, and O K-edge absorptions to 90.3%, 84.0%, and 88.7%, respectively. Hence, it is clear that a sub-millimeter gas path length is required to investigate the O K-edge as well as the higher-energy L_3-edges (i.e., the Cu L_3-edge at 932.5 eV). To maintain good signal-to-noise and overcome attenuation losses in transmission experiments, high photon brilliance and flux are necessary. The ALS and other third generation synchrotron radiation facilities meet this requirement.

The performance of the *in-situ* cell was characterized by monitoring oxidation state changes in a silica-supported Cu catalyst (3 wt. % Cu) heated in the presence of

10% O_2 or 4% CO in He, at atmospheric pressure. The catalyst was prepared by reaction of CuCl vapor with the silanol groups of mesoporous silica, SBA-15.[19] A detailed description of the preparation and characterization of this catalyst is given in references 20-21.

By touching the window surface repeatedly to a small quantity of the catalyst, particles estimated at ~ 1-10 ng were deposited onto the front side of a Si_3N_4 window. The smallest particles adhered by static forces. The window was inspected with a visual light microscope and then attached to the front side of the cell. The cell was then positioned in the STXM and electrical and gas connections made as shown in Figure 3.

Prior to acquiring data, the chamber housing the STXM was sealed under ambient atmospheric conditions and the reactor flow channels (including the catalyst particles) were purged with He at room temperature. Cu L_3 images were recorded on beam line 11.0.2 of the ALS[22]. The X-ray flux (typically 10^{12} photons/s) transmitted through the sample impinged on a phosphor and the resulting photons were photon counted with a photomultiplier. With the ALS storage ring running at 1.9 GeV and 350 mA, count rates were 1-2 MHz.[14,22] For line scans, dwell times ranged from 0.3-2.0 ms per pixel, and were 0.8 ms per pixel for the image scans. The spatial resolution of the microscope was approximately 40 nm. The monochromator has no entrance and exit slits, hence slits prior to the STXM were set such that the energy resolution was approximately 250 meV at the Cu L_3 edge. Horizontally polarized light was used and the polarization was not varied in these experiments.

An overview image of the sample (200 μm x 200 μm) was obtained just below the Cu L_3-edge, at 926.0 eV, by scanning the cell relative to the X-ray beam (Figure 4a).

Successively smaller areas at higher resolution were imaged at the same energy to locate a Cu catalyst particle of appropriate thickness. This particle was then followed over the course of the entire reaction. A particle image was acquired at successive energy steps (see for example Figure 4b) to produce a series of images referred to as a "stack." Stack measurements were done with 12 μm x 12 μm images at a spatial resolution of 100 nm per pixel (0.8 ms dwell per pixel) with energy steps of 0.25 eV over the energy range 926.0 to 937.0 eV. A stack was acquired in approximately 15 min. After data acquisition, the images in the stack were aligned to account for any small changes in the sample position by performing a spatial cross-correlation analysis.[23] Such changes were minor in these experiments. After stack alignment, the images were analyzed using AXIS software to extract an energy spectrum from any pixel or group of pixels in the image stack.[23]

Figure 4a shows the image of the sample obtained with a 200 μm x 200 μm scan at 926.0 eV. The darker areas correspond to particles of silica-supported Cu. An individual catalyst particle, of appropriate thickness to lie within the linear regime of Beer's law, was then chosen for further analysis (see the dotted outline in Figure 4a). Individual images from stacks taken at 308 K, 353 K, 403 K and 473 K in 4% CO of this catalyst particle are shown in Figure 4b-e. The energy of 931.4 eV corresponds to a strong absorption characteristic for the 2p→3d transition of Cu(II).[24] With increasing temperature the intensity of the particle image decreases due to reduction of CuO by CO. Upon switching from 4% CO to 10% O_2 at 473 K followed by cooling in the presence of the O_2 to 308 K, the intensity of the catalyst particle image is restored, indicating the reoxidation of Cu (Figure 4f).

The absorbance A, as a function of energy for the particle imaged in Figure 4 is given by

$$A = ln\ (\bar{I}_0/\bar{I}), \quad (1)$$

where $\bar{I}_0$ and $\bar{I}$ correspond to the integrated intensity over a region of the window free of particles and a region occupied by a particle (see Figure 4b). Equivalent areas of the two regions are chosen such that Beer's law is valid and resulted in an absorbance of 0.7 at 926.0 eV. [25]

The absorption spectrum at each temperature, without normalization, is shown in Figure 5. Background absorption was subtracted from each spectrum by fitting a straight line through the endpoints of the data set. The strong absorption peak at 931.4 eV is characteristic of Cu(II).[24] The small peak at 934.7 eV, characteristic of Cu(I), suggests that even at room temperature CO reduces Cu(II) to Cu(I) (Figure 5a). Similar effects for supported Cu were observed by IR spectroscopy of adsorbed CO.[26] At 403 K, the Cu(II) peak loses intensity relative to its initial intensity and the Cu(I) broadens and shifts to lower energies (Figure 5b). Even at 473 K (Figure 5c), the Cu(II) peak intensity is still noticeable, while the Cu(I) intensity increases. The subtle shifts in peak position of Cu(II) and Cu(I) may be an indication of slight changes in the local environment of the absorbing copper center. More detailed studies are necessary to understand these phenomenon. Upon reoxidation, the Cu(II) peak regains intensity but does not return to its original intensity prior to oxidation (Figure 5d).

Discussion

To obtain quantitative data in transmission mode requires samples of uniform thickness. In the present case, the small amount of catalyst powder distributed on the Si_3N_4 window contains a distribution of particle sizes and thicknesses. A transmission experiment performed with an unfocused beam illuminating the entire sample window will be plagued by pinhole effects and other nonlinear thickness variations making the absorption data non-quantitative.[2] This problem can be overcome by locating a single particle of uniform thickness. This feature of the STXM enables one to determine variations in oxidation state quantitatively, as shown here for the case of silica-supported copper. While the results reported here were taken under steady state conditions, it is also possible to acquire data under dynamic conditions in which the time scale of the dynamics are commensurate with the time scale required to acquire signals while maintaining sufficient signal-to-noise ratios.

The *in-situ* cell described here was designed specifically to meet the constraints of the STXM at the ALS, but it is not restricted to the STXM apparatus. With minor modification, this cell could be adapted to fluorescence mode measurement using unfocused beamlines at the ALS or other SR facilities. Future studies will include efforts in the direction of fluorescence detection and to modify the materials used for cell construction to permit operation at temperatures higher than 533 K.[27]

Acknowledgements

The authors would like to thank the ALS BL 11.0.2 team for their support and willingness to allocate beam line commissioning time to this project. This work was supported by the Director of the Office of Science, Office of Basic Energy Sciences,

Division of Chemical Sciences, Geosciences, and Biosciences and the Division of Materials Sciences of the U.S. Department of Energy at the ALS and LBNL under Contract No. DE-AC03-76SF00098. Additional support was provided by the Methane Conversion Cooperative, funded by BP, and in part (TCNL) by the National Institutes of Health (HG01399).

References

[1]G.E. Brown, Jr., G. Calas, G.A. Waychunas, and J. Petiau, in *Spectroscopic Methods in Mineralogy and Geology, Reviews in Mineralogy*, edited by F. Hawthorne (Mineralogical Society of America, Washington, DC, 1988), Vol. 18, pp. 431-512.

[2]*X-ray Absorption: Principles, Applications, Techniques of EXAFS, SEXAFS and XANES*, edited by D.C. Koningsberger and R. Prins (Wiley, New York, 1988).

[3]*Practical Surface Analysis*, 2nd ed., edited by D. Briggs and M.P. Seah (Wiley, New York, 1990), Vol. 1.

[4]J. Stöhr, *NEXAFS Spectroscopy* (Springer, Berlin, 1992).

[5]S. Schroeder, G. Moggridge, R. Lambert, and T. Rayment, in *Spectroscopy for Surface Science*, edited by R. Clark and R. Hester (Wiley, New York, 1998), pp. 1-69.

[6]D. Bazin, H. Dexpert and J. Lynch, in *X-ray Absorption Fine Structure for Catalysts and Surfaces,* edited by Y. Iwasawa (World Scientific, Singapore, 1996), p. 113.

[7]A.M.J. van der Eerden, J.A. van Bokhoven, A.D. Smith, and D.C. Koningsberger, Rev. Sci. Instrum. **71**, 3260 (2000).

[8]F.M.F de Groot, Top. Catal. **10**, 179 (2000).

[9]W.M. Heijboer, A.A. Battiston, A. Knop-Gericke, M. Hävecker, R. Mayer, H. Bluhm, R. Schlögl, B.M. Weckhuysen, D.C. Koningsberger, and F.M.F de Groot, J. Phys. Chem. B **107**, 13069 (2003).

[10]A. Knop-Gericke, M. Hävecker, Th. Neisius, and T. Schedel-Niedrig, Nucl. Instrum. Methods Phys. Res. A **406**, 311 (1998).

[11]D.F. Ogletree, H. Bluhm, G. Lebedev, C.S. Fadley, Z. Hussain, and M. Salmeron, Rev. Sci. Instrum. **73**, 3872 (2002).

[12]A.T. Bell, Science **299**, 1688 (2003).

[13] P.M. Bertsch, D.B. Hunter, Chem. Rev. **101**, 1809 (2001).

[14]A.L.D. Kilcoyne, T. Tyliszczak, W.F. Steele, S. Fakra, P. Hitchcock, K. Franck, E. Anderson, B. Harteneck, E.G. Rightor, G.E. Mitchell, A.P. Hitchcock, L. Yang, T. Warwick and H. Ade, J. Synchrotron Rad. **10**, 125 (2003).

[15]P. C. Simpson, A. T. Woolley, and R. A. Mathies, Biomedical Microdevices **1**, 7 (1998).

[16]W.H. Grover, A.M. Skelley, C.N. Liu, E.T. Lagally, R.A. Mathies, Sens. Actuat. B **89**, 315 (2003).

[17]A graphical instrument control environment developed by National Instruments, Inc., Austin, TX. (http://www.ni.com)

[18]Values were calculated using the web interface of the Center for X-ray Optics at Lawrence Berkeley National Laboratory, Berkeley, CA: http://www-cxro.lbl.gov/optical_constants/pert_form.html.

[19]D. Zhao, J. Feng, Q. Huo, N. Melosh, G.H. Fredrickson, B.H. Chmelka, and G.D. Stucky, Science **279**, 548 (1998).

[20]I. Drake, K.L. Fudala, S. Baxamusa, A.T. Bell and T.D. Tilley, J. Phys. Chem. B (unpublished).

[21]I. Drake, K.L. Fudala, A.T. Bell and T.D. Tilley, J. Catal. (unpublished).

[22]T. Tyliszczak, T. Warwick, A.L.D. Kilcoyne, S. Fakra, D.K. Shuh, T.H. Yoon, G.E. Brown, Jr., S. Andrews, V. Chembrolu, J. Strachan and Y Acermann, in Eighth International Conference on Synchrotron Radiation Instrumentation, AIP Conference Proceedings, **705**, 1356 (2004).

[23]AXIS software: Data Analysis program available from A. Hitchcock and C. Jacobsen (http://unicorn.mcmaster.ca/aXis2000.html).

[24]L.H. Tjeng, C.T. Chen, J. Ghijsen, P. Rudolf, and F. Sette, Phys. Rev. Let. **67**, 501 (1991).

[25]K. Pecher, D. McCubbery, E. Kneedler, J. Rothe, J. Bargar, G. Meigs, L. Cox, K. Nealson, and B. Tonner, Geochim. Cosmochim. Acta **67**, 1089 (2003).

[26]K. Hadjiivanov, T. Tsoncheva, M. Dimitrov, C. Minchev, and H. Knözinger, App. Catal. A **241**, 331 (2003).

[27]Towards this effort, a more robust version of the *in-situ* cell has been made using glass-glass microchannels formed by thermally bonding of the drilled channel wafer to a 210 μm blank wafer rather than use of PDMS bonding which limits the temperature range studied. Glass-glass bonding was achieved using a programmable vacuum furnace (Centurion VPM, J.M. Ney, Yucaipa, CA) at 853 K for 4 hours. Aluminum was then deposited and patterned on the bonded wafer to form the resistive heater.

Figure Captions

FIG. 1. (a) Drawing of micro fabricated reactor showing details of the heater, channels and PDMS layers. (b) Cross section of cut represented by dotted line in (a). The vertical dimensions are to scale, while the horizontal dimension are not, allowing details to be more easily examined. (c) Picture of *in-situ* cell with all necessary components. The gas tube fittings, Al plasma etched heater, thermocouple wire, and Si_3N_4 window (3 mm window on 7 x 7 mm Si frame) are clearly visible.

FIG. 2. Calculated absorption[18] due to two 100 nm thick Si_3N_4 windows and three complex gas mixtures (4 % CO, and 10% O_2, 12 % CO, and 30% O_2, 20 % CO, and 50% O_2). The X-ray path length was set to 0.8 mm.

FIG. 3. (a) Picture of microreactor positioned within STXM. The heater contact clips and strain plate for gas and electrical connections are visible. (b) CAD drawing showing more clearly peripheral components and size constraints.

FIG. 4. Spectromicroscopy images of the 3 wt. % Cu on SiO_2 deposited on the Si_3N_4 window of the *in-situ* cell under varying reaction conditions. Regions of strong contrast are due to the sample particles, while all other regions contain no particles and are mass absorption of the Si_3N_4 windows. (a) Particles in a 200 μm x 200 μm field of view at 926.0 eV, dotted box indicates the specific particle used to obtain Cu L_3-edge absorption spectra. (b) Magnified image (12 μm x 12 μm) of particle identified by dotted box in (a). Image shows regions used for I_0 (outlined circle) and I (dash-dot). Identical regions were

used for all subsequent images. (b)-(e) Identical particle followed through temperature ramp up to 473 K in 4% CO. (f) Image of identical particle after subsequent oxidation in 10% O_2. Images in (a)-(f) are of a single frame of each stack image at 931.4 eV.

FIG. 5. Cu L_3-edge spectra of a single particle at various temperatures and gas compositions. (a)-(c) 4% CO (in He) at 308 K, 403 K, and 473 K. (d) Spectrum taken at 308 K after cooling cell at 5 K min^{-1} (from 473 K) in 10% O_2 (in He).

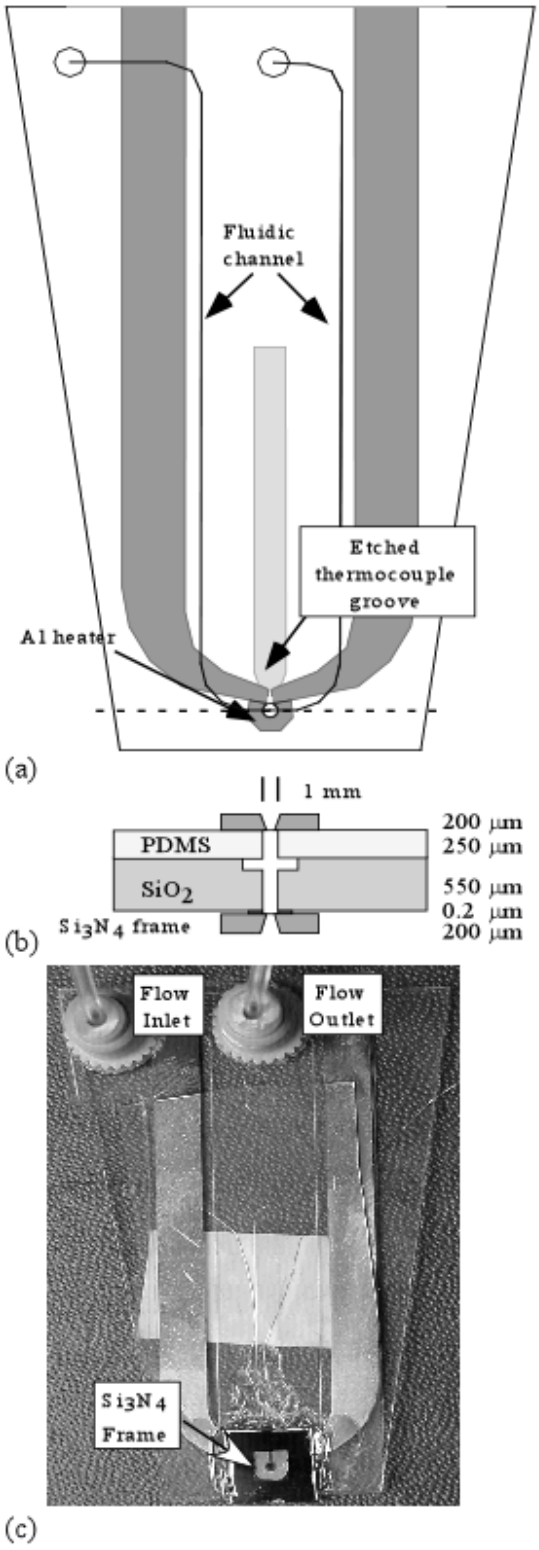

Figure 1, Ian Drake, *Review of Scientific Instruments*

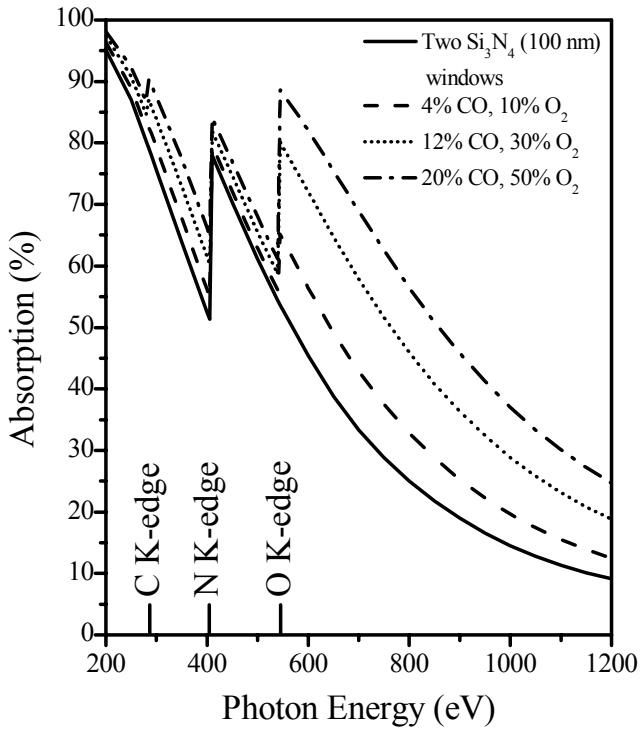

Figure 2, Ian Drake, *Review of Scientific Instruments*

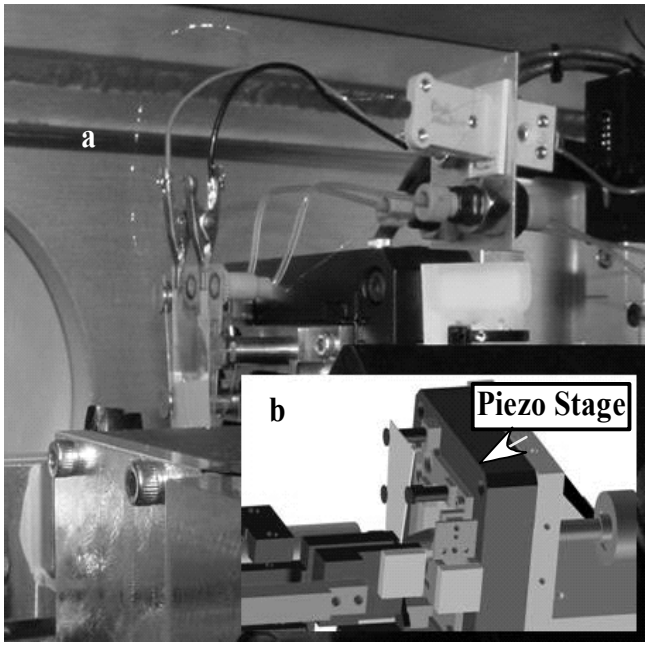

Figure 3, Ian Drake, *Review of Scientific Instruments*

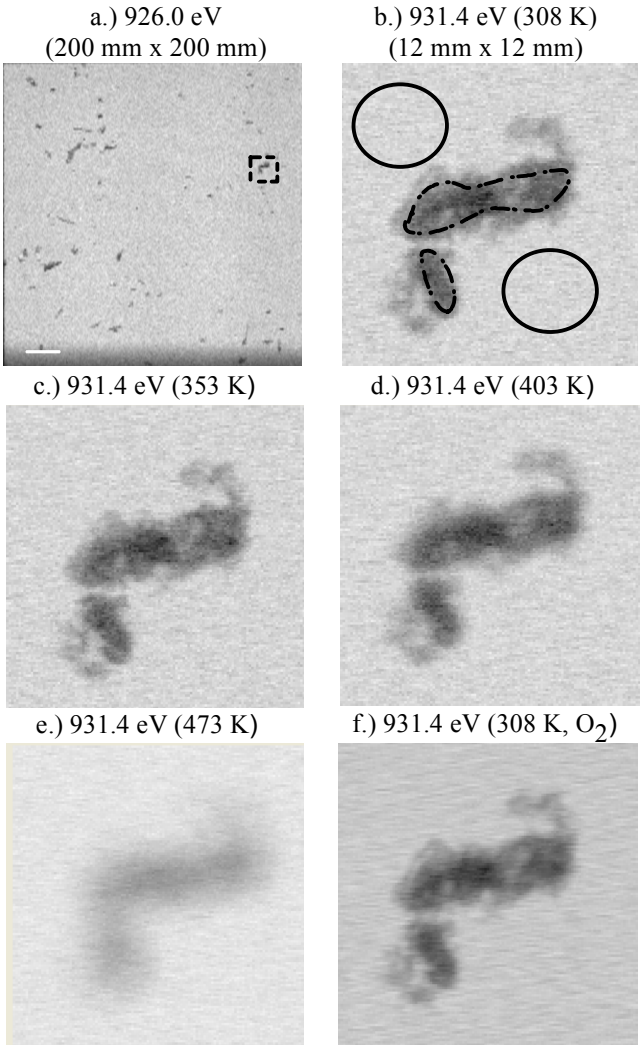

Figure 4, Ian Drake, *Review of Scientific Instruments*

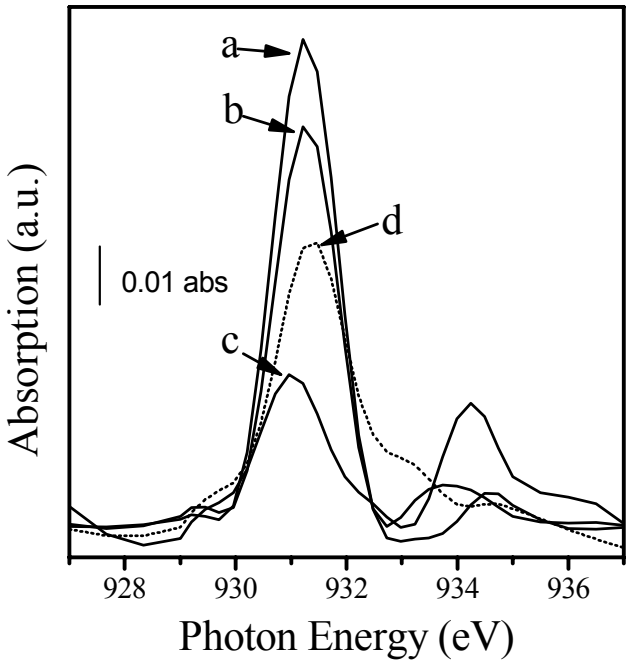

Figure 5, Ian Drake, *Review of Scientific Instruments*